Available online at www.HighTechJournal.org

HighTech and Innovation Journal

Vol. 7, No. 1, March, 2026

ISSN: 2723-9535

A Data-Driven SPC Framework for Monitoring and Forecasting Global Temperature Trends

Yadpirun Supharakonsakun [1*], Korakoch Silpakob [2], Yupaporn Areepong [3]

[1] *Department of Applied Mathematics and Statistics, Faculty of Science and Technology, Phetchabun Rajabhat University, 67000 Phetchabun, Thailand.*

[2] *Department of Educational Testing and Research, Faculty of Education, Buriram Rajabhat University, 31000 Buriram, Thailand.*

[3] *Department of Applied Statistics, Faculty of Applied Science, King Mongkut's University of Technology North Bangkok, Bangkok 10800, Thailand.*

Received 21 April 2025; Revised 23 January 2026; Accepted 01 February 2026; Published 01 March 2026

Abstract

This study aims to develop an enhanced Statistical Process Control (SPC) framework for the effective monitoring and forecasting of global temperature trends, addressing the limitations of traditional control charts in handling autocorrelated environmental data. The primary objective is to construct a modified Exponentially Weighted Moving Average (EWMA) chart capable of detecting both abrupt and gradual shifts in time series exhibiting seasonal and stochastic dependencies. The proposed approach models global temperature data using a Seasonal Autoregressive Moving Average process with exponential white noise (SARMA$(1,1)_L$) to capture temporal patterns and residual variability. An analytical formulation for evaluating the one sided Average Run Length (ARL) is derived, enabling quantitative assessment of chart performance. The simulation analysis demonstrates that, by applying an optimized smoothing parameter, the proposed EWMA control chart outperforms the traditional EWMA and CUSUM charts, particularly in detecting small shifts with significantly lower ARL_1 values. The findings confirm that the proposed model effectively tracks and predicts global temperature anomalies with high sensitivity and accuracy. The novelty of this research lies in integrating SARMA-based modeling with SPC design to improve detection reliability under autocorrelated and nonstationary conditions. This data-driven framework offers a promising tool for real-time environmental monitoring and climate forecasting applications.

Keywords: Statistical Process Control; Global Temperature; Forecasting; Monitoring; Average Run Length.

1. Introduction

The consequences of climate change can be observed in the increasing occurrence of natural disasters, including earthquakes, tsunamis, thunderstorms, floods, and landslides, which pose significant threats worldwide. Evidence for global warming is provided in the form of extreme weather events, which indicate global variability [1]. NASA reported that one of the 16 warmest years in the past 134 years occurred in 2000, highlighting increasing temperatures (NASA, n.d.). Research studies indicate that global temperatures have been increasing since the mid-1900s as a consequence of rising greenhouse gas emissions, causing spatial and seasonal changes [2]. Projections indicate that global surface temperatures could rise by at least 1.4 °C during the present century, and potentially by as much as 5.8 °C [3], posing a significant challenge for the future. Global warming can be caused by two main types of factors, comprising those that are natural in origin, including changes in solar effects or the orbit of the Earth, as well as volcanic emissions, which have only modest impacts on the global environment [4, 5], and those that have human causes, such as activities which

* Corresponding author: yupaporn.a@sci.kmutnb.ac.th

https://doi.org/10.28991/HIJ-2026-07-01-013

lead to the increased emission of carbon dioxide and other greenhouse gases, or harmful environmental practices including deforestation [6]. The accumulation of greenhouse gases in the atmosphere is a notable problem since heat is trapped, leading to an inevitable rise in temperatures. As a result, heat waves increase in duration and intensity, while drought conditions become more common. Moreover, storms are also intensified, with heavy rainfall and hurricanes presenting a growing threat.

Experts have confidently linked certain weather patterns, such as heat waves, to the long-term influence of global warming (National Academies of Science, Engineering, and Medicine, n.d.). Climate change presents a wide range of significant challenges, with melting glaciers raising sea levels by an average of 0.19 meters per year between 1901 and 2010 [7]. Coastal flooding is occurring, and many plant and animal species, including coral reefs and grasslands, are at risk of extinction. Projections indicate that, by 2060, flooding will present a major threat to at least 1.6 billion people [8]. In addition, increased air pollution is causing infectious diseases, allergies, and outbreaks of asthma. The expansion of mosquito-infested areas has increased the spread of malaria and dengue fever, among other insect-borne diseases [9]. Continuous monitoring and control of global temperature changes is essential to meet these challenges.

In order to perform quality control operations, Statistical process control (SPC) allows process changes to be monitored and controlled through a statistical approach. A key role in such procedures can be played by control charts, which serve to identify and prevent errors within an area of interest. To ensure that the process remains within acceptable limits over time, numerous studies have documented continued temperature increases, sea level rise, and changes in global precipitation patterns over the past few decades. Vucijak et al. [10] used SPC principles to assess these observed changes statistically. Their findings suggest that assessments of climate-related changes in total monthly precipitation are statistically predictable.

Vucijak et al. [11] also proposed tracking statistically significant changes and changes that exceeded expected levels. This approach is particularly relevant for assessing changes in precipitation patterns from data covering the period 1961–1990 and beyond. Control charts have also been used to monitor environmental data, such as water quality [12], air quality [13], industrial production, and bird communities in the Canadian oil sands region, using statistical control procedures [14]. Data values often exhibit autocorrelation in ecological or environmental statistical applications, indicating a relationship between current and past values [15, 16]. Deviations from the assumption of independence and normal distribution [17] in traditional control chart methods can hinder the effectiveness of Shewhart control charts when applied to such autocorrelation observations. The sequential nature of regularly recorded data points for variables over time makes detecting process changes challenging. To address this issue, researchers have proposed alternative control charts, including cumulative sum (CUSUM) charts [18] as well as exponentially weighted moving average (EWMA) charts [19], which are more suitable for normal and autocorrelated observations [20]. Among these charts, EWMA charts have been recommended due to their robust performance, especially for observations that deviate from a normal distribution or exhibit non-normal autocorrelation [21-25]. Their ability to handle non-normally distributed and correlated data makes them a valuable option for various applications.

To assess control chart effectiveness, comparative studies can be performed on the basis of average operating length (ARL), which serves as a measure of the capacity of a control chart for effective change detection in the context of process averages [26-28]. Several techniques can be applied for ARL determination, such as the Markov Chain method [29-31], Monte Carlo simulation [32, 33], Martingale technique, and NIE (numerical integral equations) approach [34], along with the explicit formula. The accuracy offered by the explicit formula in determining the ARL value accounts for its widespread use.

The Average Run Length (ARL) is widely recognized as a critical performance metric in Statistical Process Control (SPC), providing a quantitative measure of how quickly a control chart detects shifts in process behavior. Among the various analytical and computational techniques developed to estimate ARL, the explicit formula approach has been proven to be particularly advantageous due to its mathematical precision, reduced computational burden, and consistency across different process conditions. Unlike simulation-based methods that rely on repetitive random sampling or numerical iterations, the explicit formula yields closed-form solutions that accurately capture ARL behavior, enabling efficient and reliable evaluation of control chart performance. This property makes it an attractive analytical tool for both theoretical exploration and real-time process monitoring applications.

Most existing studies have primarily relied on traditional simulation-based or numerical approaches for estimating the Average Run Length (ARL), which, although effective, often demand considerable computational effort and exhibit limited adaptability to complex autocorrelated structures. Furthermore, explicit analytical formulations of ARL have received relatively little attention, particularly for data with serial dependence incorporating non-Gaussian (specifically, exponential) white noise. This represents a significant methodological gap, motivating the present study to introduce an explicit analytical ARL expression that enhances both computational precision and efficiency in process monitoring.

To address the research gap, the present study focuses on the development and evaluation of a modified Exponentially Weighted Moving Average (EWMA) control chart based on the Seasonal Autoregressive Moving Average

SARMA$(1,1)_L$ model incorporating exponential white noise. This configuration is particularly suitable for analyzing autocorrelated time series data exhibiting seasonal patterns, such as global temperature anomalies. By deriving an explicit formula for the ARL within this framework, the study aims to provide an analytically tractable yet highly accurate method for monitoring and detecting mean shifts in autocorrelated processes.

Earlier research commonly employed ARL values as the principal metric for assessing control chart robustness. However, this study advances the field by applying a modified Exponentially Weighted Moving Average (EWMA) chart to detect both subtle and abrupt mean shifts occurring in autocorrelated processes. The focus lies in formulating an explicit analytical ARL solution applicable across a diverse range of autocorrelated models, including the first-order moving average (MA(1)) [35], general moving average (MA(q)) [13], autoregressive moving average (ARMA(1,1)) [36], integrated moving average (IMA) and fractional integrated moving average (FIMA) models, as well as seasonal autoregressive (AR$(p)_L$) and seasonal moving average (SMA$(p)_L$) [37] processes with exponential white noise. Such an inclusive analytical framework enables broader applicability and enhances the theoretical generalization of the proposed chart.

To validate the accuracy of the explicit ARL formulation, the Numerical Integral Equation (NIE) method is also implemented, providing a numerical benchmark for verification. The close agreement between the explicit and numerical results not only confirms the robustness of the proposed derivation but also underscores its computational efficiency compared to iterative or simulation-based approaches. This two-step validation ensures that the analytical solution maintains both mathematical rigor and practical reliability.

This study also extends the use of the modified EWMA chart to environmental and climatological monitoring, demonstrating its enhanced ability to detect or predict structural shifts in global temperature time series. A comprehensive comparative performance evaluation is conducted, contrasting the proposed chart with classical EWMA and CUSUM schemes under various mean-shift conditions to establish its superior detection capability and efficiency.

The remainder of this paper is structured as follows: Section 2 introduces the principles of statistical process monitoring using control charts, providing the theoretical foundation for process stability assessment. Section 3 describes the proposed methodology for evaluating mean shift detection and developing both the explicit ARL and numerical integral equation (NIE) solutions. Section 4 presents the numerical results, highlighting the comparative performance of the modified EWMA chart under various shift conditions. Section 5 demonstrates the application of the proposed framework to real-world global temperature data, illustrating its practical relevance and forecasting capability. Section 6 discusses the findings and interprets their broader implications for process monitoring and climate analytics. Finally, Section 7 concludes the paper with key insights, contributions, and recommendations for future research.

2. Statistical Process Monitoring Using Control Charts

In order to examine the performance of a process over a period of time, control charts can be employed. These serve as a statistical process control (SPC) tool, which represents data in a visual format, enabling the tracking of specific metrics related to performance so that the observer can assess whether or not a process remains in control; that is, the data remain within acceptable bounds. The key function of a control chart is to determine whether variations in the data are within the range of normal expectations or can be considered as unexpected deviations that demand corrective action to be taken.

Among the main advantages offered by a control chart is the capacity to identify potential problems early on. Control charts provide the opportunity to detect and correct issues before they become severe by monitoring process performance in real time, thus preventing costly errors. They also help to reduce variation within the process, resulting in more consistent and reliable results.

Differing forms of data or observation requirements necessitate the design of differing control charts. Among the various types, the EWMA (Exponentially Weighted Moving Average) chart is especially useful in identifying minor changes in process means, allowing it to be used to stabilize procedures where small changes can cause large effects. The EWMA chart was first proposed by Roberts [19], noting its capacity for detecting subtle shifts in the performance of a monitored process. The strength of the chart design lies in its main parameters, which are the control limit width along with the smoothing parameter. The EWMA statistic, denoted byZ_t, can be defined as shown below:

$$Z_t = (1-\lambda)Z_{t-1} + \lambda Y_t, \tag{1}$$

in which $0 < \lambda \leq 1$ defines the smoothing parameter, while Y_t, $t = 1, 2, 3, \ldots$ indicates a series of autocorrelated observations. The starting value for Z_0 matches the target mean of the process as μ_0.

Upper and lower control limits are determined for the control chart, with definitions given as:

$$UCL = \mu_0 + L\sigma\sqrt{\frac{\lambda}{2-\lambda}[1-(1-\lambda)^{2t}]}, \tag{2}$$

$$LCL = \mu_0 - L\sigma\sqrt{\frac{\lambda}{2-\lambda}[1-(1-\lambda)^{2t}]}, \quad (3)$$

in which the multiplier, L, indicates the width of the control limit, while the standard deviation for the process is given by σ. When the value of t increases, the term $(1-\lambda)^{2t}$ approaches 0, which results in the upper and lower control limits converging towards their steady-state values. Specifically, as $t \to \infty$, the control limits simplify to:

$$UCL = \mu_0 + L\sigma\sqrt{\frac{\lambda}{2-\lambda}}, \quad (4)$$

$$LCL = \mu_0 - L\sigma\sqrt{\frac{\lambda}{2-\lambda}}, \quad (5)$$

To address certain limitations of the original EWMA chart, particularly its inertia and delayed detection of changes, Patel & Divecha [38] proposed modifications to the original EWMA control chart in order to address the problem of inertia due to EWMA statistic errors. The approach works through the incorporation of the latest observation value along with past changes in the process. This modified approach has been shown to allow the identification of process shifts that arise in both autocorrelated observations and those that follow an independent normal distribution.

Building on these advancements, an alternative control statistic was suggested by Khan et al. [39] on the basis of a modified EWMA framework. Their approach adjusts the structure of the EWMA statistic as follows:

$$Z_t = (1-\lambda)Z_{t-1} + \lambda Y_t + c(X_t - X_{t-1}), \quad (6)$$

in which the smoothing parameter is indicated by λ, the autocorrelated observations are shown as X_t, $t = 1, 2, 3, ...$, and the constant, c, refers to a further adjustment. The statistic has an initial value which matches the target mean of the process,μ_0, in line with the approach of the original EWMA model. However, the final term is expanded to incorporate additional process information, enhancing its effectiveness in monitoring changes.

The modified EWMA control chart will produce either a signal denoting 'out-of-control' or a false alarm when its value surpasses the predetermined control limits. The general expressions for the upper and lower control limits for this particular modified EWMA chart can be expressed as:

$$UCL = \mu_0 + H\sigma\sqrt{\frac{\lambda+2c\lambda+2c^2}{2-\lambda}}, \quad (7)$$

and

$$LCL = \mu_0 - H\sigma\sqrt{\frac{\lambda+2c\lambda+2c^2}{2-\lambda}}, \quad (8)$$

in which the width of the control limit is denoted by H, and the process standard deviation is shown by σ. The process of shift detection becomes much more sensitive when this revised structure is used, improving the traditional EWMA by mitigating potential errors in monitoring.

3. Methods for Evaluating Mean Shifts Detection

This paper introduces a modified EWMA process capable of improving the observation and identification of abrupt yet small alterations in autocorrelated data. The proposed modification increases the sensitivity of the standard EWMA, making it particularly effective in environments where early detection of shifts in process performance is essential. Evaluating the effectiveness of this modified EWMA requires the use of calculations for the Average Run Length (ARL), a key metric for assessing control chart performance. Specifically, we present an explicit analytical derivation of ARL for a first-order seasonal autoregressive moving average (SARMA$(1,1)_L$) procedure incorporating white noise with an exponential distribution, improving accuracy in detecting shifts within autocorrelated processes.

Although the SARMA$(1,1)_L$ model assumes weak stationarity, the proposed framework addresses the non-stationary behavior commonly observed in temperature data by applying seasonal differencing and incorporating an adaptive EWMA smoothing parameter. This design allows the modified EWMA chart to remain robust under gradual or long-term trends, such as global warming, while maintaining sensitivity to short-term deviations.

In this study, the time series analysis plays a crucial role in understanding autocorrelated data. A time series consists of sequentially collected data points observed at specific time intervals, with the primary goal of predicting future values when the independent variable is time. Autocorrelation plays a key role in time series data, representing links between data observations arising at different time points within the dataset. Autocorrelated data reflects the extent of similarity between observations based on the time interval separating them.

For univariate time series modeling, the SARMA$(1,1)_L$ process is a commonly applied method that combines aspects of both the autoregressive (AR) and moving average (MA) approaches. This process is particularly useful in scenarios where the current observation is influenced by its immediate past values and residual errors from previous time points.

By combining the SARMA(1,1)$_L$ model with the modified EWMA mechanism, the proposed method effectively captures both short-term autocorrelation and long-term structural changes, providing a stable and responsive monitoring tool for non-stationary temperature series. Formally, the model can be represented as:

$$Y_t = \mu + \varphi Y_{t-L} - \theta \varepsilon_{t-L} + \varepsilon_t, \tag{9}$$

where μsignifies the time series model mean, $\varepsilon_t$denotes the process of white noise that follows an exponential distribution, φ stands for the autoregressive coefficient, and $\theta$is the coefficient for the moving average process. The combination of AR and MA terms allows the model to account for both the momentum from past values and the impact of previous errors, making it a versatile tool in time series forecasting.

Therefore, the modified EWMA statistic for the SARMA(1,1)$_L$ model can be expressed as:

$$Z_t = (1-\lambda)Z_{t-1} + (\lambda + c)(\mu + \varphi Y_{t-L} - \theta \varepsilon_{t-L}) + (\lambda + c)\varepsilon_t - cY_{t-1}, \tag{10}$$

where $t = 1, 2, 3, ..., L$ is a period of time, while the starting value matches the process mean $Z_0 = \mu$, and $Y_0 = v$. We assume a one-sided control limit, whereby the lower control limit (LCL) is 0 and the upper control limit (UCL) is$h$), which denotes an in-control process at the time where $0 \le Y_{t-L} \le h$. Accordingly,

$$Z_1 = (1-\lambda)u + (\lambda + c)(\mu + \varphi Y_{t-L} - \theta \varepsilon_{t-L}) + (\lambda + c)\varepsilon_1 - cv, \tag{11}$$

Let ARL represent average run length for the control chart of modified EWMA. This gives the integral equation shown below:

$$ARL = 1 + \int_{\frac{-g}{\lambda+c}}^{\frac{h-g}{\lambda+c}} W\big((\lambda + c)x + g\big) f(x)dx f(w)dw, \tag{12}$$

where, $g := (1-\lambda)u + (\lambda + c)(\mu + \varphi Y_{t-L} - \theta \varepsilon_{t-L}) - cv$.

By transforming the integral variable in Equation 11, the resulting integral equation is expressed as follows:

$$ARL = 1 + \frac{1}{\lambda+c}\int_0^h f(w) f\left\{\frac{w-(1-\lambda)u}{\lambda+c} + \frac{cv}{\lambda+c} - (\mu + \varphi Y_{t-L} - \theta \varepsilon_{t-L})\right\} dw. \tag{13}$$

here, it is possible to derive the integral equation for calculating average run length (ARL) using two methods:

3.1. Explicit Formula

It is possible to make use of the Fredholm integral equation of the second kind to derive the explicit formula for the ARL (Average Run Length) of the Seasonal Autoregressive Moving Average (SARMA(1,1)$_L$) model incorporating exponential white noise using the modified EWMA control chart. The following procedure is applied since the process of white noise is distributed exponentially:

$$ARL = 1 + \frac{C(u)}{\beta_0(\lambda+c)}\int_0^h f(w) e^{\frac{-w}{\beta_0(\lambda+c)}} dw = 1 + \frac{C(u)}{\beta_0(\lambda+c)} Q, \tag{14}$$

where, $C(u) = e^{\frac{(1-\lambda)u - cv}{\beta_0(\lambda+c)} + \frac{1}{\beta_0}(\mu + \varphi Y_{t-L} - \theta \varepsilon_{t-L})}$ and

$$\begin{aligned}
Q &= \int_0^h L(w) e^{\frac{-w}{\beta_0(\lambda+c)}} dw \\
&= \int_0^h \left[1 + \frac{Q}{\beta_0(\lambda + c)} C(w)\right] e^{\frac{-w}{\beta_0(\lambda+c)}} dw \\
&= \int_0^h e^{\frac{-w}{\beta_0(\lambda+c)}} dw + \int_0^h \frac{Q}{\beta_0(\lambda + c)} C(w) \cdot e^{\frac{-w}{\beta_0(\lambda+c)}} dw \\
&= \int_0^h e^{\frac{-w}{\beta_0(\lambda+c)}} dw + \int_0^h \frac{Q e^{\frac{(1-\lambda)w - cv}{\beta_0(\lambda+c)} + \frac{1}{\beta_0}(\mu + \varphi Y_{t-L} - \theta \varepsilon_{t-L})}}{\beta_0(\lambda + c)} \cdot e^{\frac{-w}{\beta_0(\lambda+c)}} dw \\
&= -\beta_0(\lambda + c)\left(e^{\frac{-h}{\beta_0(\lambda+c)}} - 1\right) + \frac{Q e^{\frac{-cv}{\beta_0(\lambda+c)} + \frac{1}{\beta_0}(\mu + \varphi Y_{t-L} - \theta \varepsilon_{t-L})}}{\beta_0(\lambda + c)} \int_0^h e^{\frac{-\lambda w}{\beta_0(\lambda+c)}} dw
\end{aligned}$$

$$= \frac{-\beta_0(\lambda+c)\left(e^{\frac{-h}{\beta_0(\lambda+c)}}-1\right)}{1+\frac{e^{\frac{-cv}{\beta_0(\lambda+c)}+\frac{1}{\beta_0}(\mu+\varphi Y_{t-L}-\theta\varepsilon_{t-L})}}{\lambda}\left(e^{\frac{-\lambda h}{\beta_0(\lambda+c)}}-1\right)},$$

Therefore,

$$ARL = 1+\frac{e^{\frac{(1-\lambda)u-cv}{\beta_0(\lambda+c)}+\frac{1}{\beta_0}(\mu+\varphi Y_{t-L}-\theta\varepsilon_{t-L})}}{\beta_0(\lambda+c)}\cdot\frac{-\beta_0(\lambda+c)\left(e^{\frac{-h}{\beta_0(\lambda+c)}}-e^{\frac{-g}{\beta_0(\lambda+c)}}\right)}{1+\frac{e^{\frac{-cv}{\beta_0(\lambda+c)}+\frac{1}{\beta_0}(\mu+\varphi Y_{t-L}-\theta\varepsilon_{t-L})}}{\lambda}\left(e^{\frac{-\lambda h}{\beta_0(\lambda+c)}}-e^{\bar{\beta}}\right.} \quad (15)$$

As a result, the Fredholm integral equation of the second kind can be employed to represent the explicit formula of the one-sided ARL of the seasonal autoregressive moving average (SARMA(1,1)$_L$) process incorporating exponential white noise using the modified EWMA control chart. The equation is shown as:

$$ARL = 1-\frac{\lambda e^{\frac{(1-\lambda)u}{\beta_0(\lambda+c)}}\left[e^{-\frac{h}{\beta_0(\lambda+c)}}-1\right]}{\lambda e^{\frac{-\mu}{\beta_0}}\cdot e^{\frac{-(\lambda\varphi+\varphi-1)Y_{t-L}-cv}{\beta_0(\lambda+k)}}\cdot e^{\frac{(\lambda\theta+\theta)\varepsilon_{t-L}}{\beta_0(\lambda+k)}}+\left[e^{\frac{-\lambda h}{\beta_0(\lambda+c)}}-1\right]}, \quad (16)$$

where ARL is characterized in the case of both in-control and out-of-control states, where the in-control parameter β_0 and the out-of-control process parameters $\beta_1 > \beta_0$determine the control conditions.

3.2. Numerical Integral Equation (NIE)

The integral equation shown in (13) serves as the basis for the application of the Numerical Integral Equation (NIE) approach, which allows the equation to be solved via application of the Gauss-Legendre quadrature rule, as demonstrated below.

$$L(a_i) = 1+\frac{1}{\lambda+c}\sum_{j=1}^{m} w_j L(a_j) f\left(\frac{a_j-(1-\lambda)u}{\lambda+c}+\frac{cv}{\lambda+c}-\mu+\varphi Y_{t-L}-\theta\varepsilon_{t-L}\right), \quad (17)$$

where, $i = 1, 2, 3, ..., m$, $a_j = \frac{b-a}{m}\left(j-\frac{1}{2}\right)+a$, and $j = 1, 2, 3, ..., m$.

This can be rewritten in matrix form as follows.

$$L_{m\times 1} = (I_m - R_{m\times m})^{-1} 1_{m\times 1}, \quad (18)$$

where, $L_{m\times 1} = \begin{bmatrix} L(a_1) \\ \vdots \\ L(a_m) \end{bmatrix}$, $1_{m\times 1} = \begin{bmatrix} 1 \\ \vdots \\ 1 \end{bmatrix}$, I_m is the identity, $R_{m\times m} = \frac{1}{\lambda+c}\begin{bmatrix} w_1 f_{11} & \cdots & w_m f_{1m} \\ w_1 f_{21} & \cdots & w_m f_{2m} \\ \vdots & & \vdots \\ w_1 f_{m1} & \cdots & w_m f_{mm} \end{bmatrix}$, and $f_{ij} := f\left(\frac{a_j-(1-\lambda)u}{\lambda+c}+\frac{cv}{\lambda+c}-\mu+\varphi Y_{t-L}-\theta\varepsilon_{t-L}\right)$.

Thus, the NIE method provides an approximation for the average run length (ARL) as follows:

$$\tilde{ARL} = 1+\frac{1}{\lambda+c}\sum_{j=1}^{m} w_j L(a_j) f\left(\frac{a_j-(1-\lambda)u}{\lambda+c}+\frac{cv}{\lambda+c}-\mu+\varphi Y_{t-L}-\theta\varepsilon_{t-L}\right). \quad (19)$$

For a more detailed algorithmic description, including both the Explicit Formula and Numerical Integral Equation (NIE) approaches, the complete pseudocode is presented in Appendix I, Table A1. This table systematically outlines each computational step, including the calculation of Percentage Relative Accuracy (%PRA). Readers interested in replicating or extending the proposed method can refer to this pseudocode for full procedural guidance.

4. Numerical Results

To measure control chart effectiveness, Average Run Length (ARL) is commonly employed. This research made use of ARL values determined via explicit equations and subsequently validated using a Numerical Integral Equation (NIE) technique involving the SARMA(1,1)$_L$ process in order to identify changes. These methods allowed comparisons to be drawn with the modified EWMA control chart. To evaluate and compare the efficiency of the two different techniques for assessing ARL, percentage relative accuracy (%PRA) can be used, as shown:

$$\%PRA = 100-\left[\left|\frac{ARL-\tilde{ARL}}{ARL}\right|\times 100\%\right], \quad (20)$$

where ARL and $\tilde{ARL}$ are average run length values obtained from the explicit formula and NIE method, respectively.

Control chart effectiveness can be assessed for both the EWMA and CUSUM charts via comparative analysis. Several performance metrics can be analyzed, including AEQL (Average Extra Quadratic Loss) and PCI (Performance Comparison Index) [40]. AEQL calculations follow the formula given as:

$$AEQL = \frac{1}{\Delta}\sum_{\delta} \delta^2 \times ARL, \tag{21}$$

where, δ represents a specific process change, while the total number of divisions is shown as ranging from 0.01 to 1.50. For the current research, delta = 10 was chosen based on the range from δ_{min} to δ_{max}. Control charts are deemed to be most effective where the minimal AEQL values are produced.

The performance comparison index (PCI) is calculated as the ratio of a control chart's average extra quadratic loss (AEQL) to the AEQL value achieved by the control chart considered to be the most effective (recording the minimum AEQL value). In mathematical terms, this can be shown as:

$$PCI = \frac{AEQL}{AEQL_{lowest}}. \tag{22}$$

When the value for PCI is 1, this represents the maximum control chart efficiency, whereas a value greater than 1 indicates a less efficient control chart.

To illustrate the proposed methodology for deriving the Average Run Length (ARL) of the SARMA$(1,1)_L$ model under the modified EWMA control chart, a flowchart is provided in Figure 1, summarizing the overall workflow from model specification to ARL computation. This visual representation highlights the main steps of the procedure, including data preparation, parameter estimation, and ARL calculation, providing readers with a clear overview of the process.

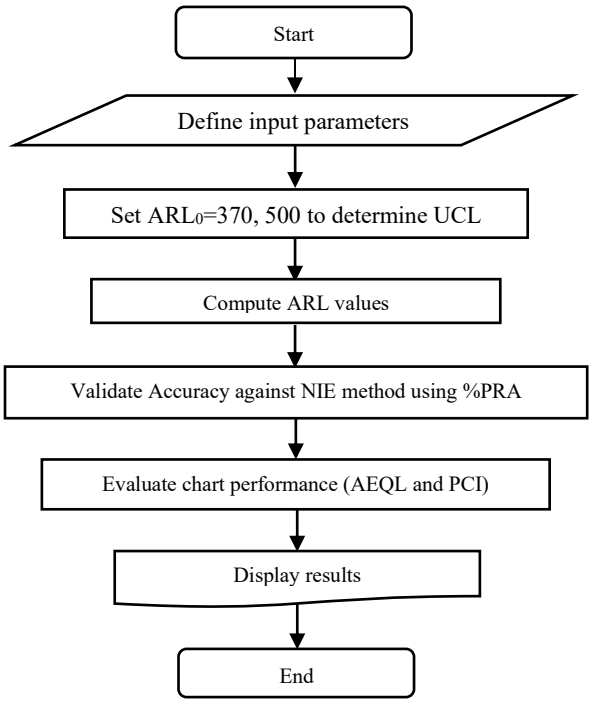

Figure 1. Workflow of Modified EWMA Control Chart for ARL Computation

When the situation is in-control, simulated data are typically given with ARL_0=370 and 500, allowing the exploration of the initial parameters at $\beta_0 = 1$. In the out-of-control scenario, the performance was analyzed to assess the response to different shift sizes by $\beta_1 = \beta_0(1 + \delta)$. Control limits, within the interval [0, h], were examined for both lower and upper bounds. The initial evaluation of ARL was completed via the explicit formula along with the Numerical Integral Equation (NIE) approach, while their capabilities were compared using the percentage relative accuracy (%PRA). The results were based on known parameters, including $(\varphi,\theta) = (0.6, 0.5), (-0.4,-0.9)$ for the SARMA$(1,1)_3$ model and $(\varphi,\theta) = (0.7, 0.8), (-0.7,-0.9)$ for the SARMA$(1,1)_4$ model. Across all models, the recommended smoothing parameter $\lambda = 0.1$ was selected to compute the control statistics for the modified control chart.

Table 1. The ARL values of the explicit formula and NIE approach for SARMA(1,1)$_3$ process when $\mu = 1$, $\lambda = 0.1$, and $c = 0.5$ on modified EWMA control chart

φ, θ	δ	ARL_0=370			ARL_0=500		
		Explicit	NIE	%PRA	Explicit	NIE	%PRA
			***h*=0.473806**			***h*=0.47492**	
$\varphi = 0.6$ $\theta = 0.5$	0.00	370.28870 (<0.001)	370.28861 (1.438)	100.00	500.06311 (<0.001)	500.06298 (1.437)	100.00
	0.01	151.48247 (<0.001)	151.48245 (1.375)	100.00	170.18800 (<0.001)	170.18797 (1.265)	100.00
	0.05	44.05740 (<0.001)	44.05739 (1.375)	100.00	45.55149 (<0.001)	45.55148 (1.421)	100.00
	0.10	22.77198 (<0.001)	22.77197 (1.515)	100.00	23.18575 (<0.001)	23.18575 (1.594)	100.00
	0.25	8.94600 (<0.001)	8.94600 (1.594)	100.00	9.01651 (<0.001)	9.01651 (1.422)	100.00
	0.50	4.43083 (<0.001)	4.43083 (1.500)	100.00	4.44944 (<0.001)	4.44944 (1.484)	100.00
	1.00	2.41506 (<0.001)	2.41506 (1.781)	100.00	2.42037 (<0.001)	2.42037 (1.469)	100.00
	1.25	2.03103 (<0.001)	2.06103 (1.5000)	100.00	2.06467 (<0.001)	2.06467 (1.593)	100.00
	1.50	1.83946 (<0.001)	1.83946 (1.250)	100.00	1.84217 (<0.001)	1.84217 (1.594)	100.00
			***h*=0.313119**			***h*=0.313927**	
$\varphi = -0.4$ $\theta = -0.9$	0.00	370.20562 (<0.001)	370.20558 (1.578)	100.00	500.20759 (<0.001)	500.20753 (1.500)	100.00
	0.01	135.56321 (<0.001)	135.56320 (1.328)	100.00	150.08356 (<0.001)	150.08355 (1.563)	100.00
	0.05	37.22680 (<0.001)	37.22680 (1.437)	100.00	38.30810 (<0.001)	38.30810 (1.765)	100.00
	0.10	18.98122 (<0.001)	18.98122 (1.547)	100.00	19.27719 (<0.001)	19.27719 (1.516)	100.00
	0.25	7.37509 (<0.001)	7.37509 (1.609)	100.00	7.42569 (<0.001)	7.42569 (2.204)	100.00
	0.50	3.66909 (<0.001)	3.66909 (1.625)	100.00	3.68268 (<0.001)	3.68268 (1.500)	100.00
	1.00	2.05933 (<0.001)	2.05933 (1.625)	100.00	2.06324 (<0.001)	2.06324 (1.578)	100.00
	1.25	1.78397 (<0.001)	1.78397 (1.641)	100.00	1.78666 (<0.001)	1.78666 (1.218)	100.00
	1.50	1.61373 (<0.001)	1.61373 (1.360)	100.00	1.61573 (<0.001)	1.61573 (1.188)	100.00

Tables 1 and 2 present the ARL values, which are calculated using both the explicit formula and the NIE method. In all cases, the acceptance rate is nearly 100%. While the explicit formula provides instant results across all scenarios, the NIE method requires approximately 1–2 seconds for computation. Therefore, utilizing the explicit formula is a more efficient approach. This indicates that the analytical approach not only reduces computational time but also achieves high numerical precision compared to the iterative NIE technique, making it particularly suitable for real-time monitoring applications where computational speed is essential. The consistency in ARL estimates between both methods further validates the correctness of the explicit formulation derived from the Fredholm integral equation.

Tables 3 and 4 show the performance of the modified EWMA (MEWMA) chart using the SARMA(1,1)$_3$ and SARMA(1,1)$_4$ models to draw comparisons with the control charts for CUSUM and EWMA, across various mean shift detection scenarios for out-of-control conditions.

Table 2. The ARL values of the explicit formula and NIE approach for SARMA(1,1)$_4$ process when $\mu = 1$, $\lambda = 0.1$, and $c = 0.5$ on modified EWMA control chart

φ, θ	δ	ARL$_0$=370			ARL$_0$=500		
		Explicit	NIE	%PRA	Explicit	NIE	%PRA
			h=0.584323			*h*=0.585619	
$\varphi = 0.7$ $\theta = 0.8$	0.00	370.25232 (<0.001)	370.25219 (1.437)	100.00	500.22470 (<0.001)	500.22449 (1.578)	100.00
	0.01	162.43580 (<0.001)	162.43577 (1.422)	100.00	183.60021 (<0.001)	183.60016 (1.313)	100.00
	0.05	48.86240 (<0.001)	48.86239 (1.516)	100.00	50.69466 (<0.001)	50.69465 (1.265)	100.00
	0.10	25.45872 (<0.001)	25.45872 (1.437)	100.00	25.97023 (<0.001)	25.97022 (1.671)	100.00
	0.25	10.04982 (<0.001)	10.04982 (1.500)	100.00	10.13662 (<0.001)	10.13662 (1.407)	100.00
	0.50	4.95887 (<0.001)	4.95887 (1.687)	100.00	4.98149 (<0.001)	4.98149 (1.609)	100.00
	1.00	2.65890 (<0.001)	2.65890 (1.687)	100.00	2.66254 (<0.001)	2.66254 (1.578)	100.00
	1.25	2.25053 (<0.001)	2.25053 (1.297)	100.00	2.25485 (<0.001)	2.25485 (1.313)	100.00
	1.50	1.99367 (<0.001)	1.99367 (1.484)	100.00	1.99688 (<0.001)	1.99687 (1.531)	100.00
			h=0.426953			*h*=0.427985	
$\varphi = -0.7$ $\theta = -0.9$	0.00	370.21045 (<0.001)	370.21039 (1.422)	100.00	500.20014 (<0.001)	500.20003 (1.438)	100.00
	0.01	147.27519 (<0.001)	147.27517 (1.593)	100.00	164.51875 (<0.001)	164.51873 (1.625)	100.00
	0.05	42.07921 (<0.001)	42.07921 (1.313)	100.00	43.44806 (<0.001)	43.44806 (1.219)	100.00
	0.10	21.67016 (<0.001)	21.67016 (1.625)	100.00	22.04799 (<0.001)	22.04799 (1.031)	100.00
	0.25	8.49019 (<0.001)	8.49019 (1.422)	100.00	8.55466 (<0.001)	8.55465 (1.531)	100.00
	0.50	4.21050 (<0.001)	4.21050 (1.486)	100.00	4.22760 (<0.001)	4.22760 (1.453)	100.00
	1.00	2.31234 (<0.001)	2.31234 (1.406)	100.00	2.31724 (<0.001)	2.31724 (1.594)	100.00
	1.25	1.98102 (<0.001)	1.98102 (1.422)	100.00	1.98439 (<0.001)	1.98439 (1.907)	100.00
	1.50	1.77426 (<0.001)	1.77426 (1.77426)	100.00	1.77676 (<0.001)	1.77676 (1.344)	100.00

Table 3 presents findings that suggest that the lowest ARL$_1$ values for each of the various situations could be observed for the MEWMA chart. This compared favorably with the CUSUM and EWMA control charts, especially in the context of lower shift sizes ($\delta \leq 0.5$) in the SARMA(1,1)$_3$ process. This result highlights the enhanced responsiveness of the modified chart, which effectively detects small but meaningful mean deviations that may go unnoticed in traditional charts. The superior performance for smaller δ demonstrates that the smoothing mechanism incorporated in the MEWMA design optimally balances sensitivity and robustness, a critical factor in climate-related data where subtle variations often signal significant environmental shifts.

The Performance Comparison Index (PCI) for the MEWMA chart reached 1.000 in nearly all cases, though, with the SARMA(1,1)$_4$ model at an ARL$_0$=370, the performance of the standard EWMA chart offered slight improvements over the proposed MEWMA scheme. This minor deviation suggests that traditional EWMA may still perform competitively under certain periodic or seasonal dependencies. However, the MEWMA's consistently lower ARL$_1$ and stable PCI confirm its reliability and overall dominance across varying process dynamics.

Similarly, Table 4 demonstrates that the MEWMA chart maintained superior detection performance with the lowest ARL1 values relative to CUSUM and EWMA in nearly all scenarios, especially for smaller shift sizes ($\delta \leq 0{,}5$) in the SARMA(1,1)$_4$ process. The PCI for the MEWMA chart was 1.000 across all cases in this table, underscoring its effectiveness in promptly detecting mean shifts. The uniform PCI of 1.000 across different seasonal models confirms that the proposed approach consistently achieves maximal control efficiency. This implies that the MEWMA chart can effectively serve as a robust statistical monitoring tool for autocorrelated and seasonally fluctuating data, such as global temperature anomalies, providing both precision and adaptability over long-term observations.

Table 3. Calculated ARL values using the explicit formula for the SARMA(1,1)$_3$ process in the case of $\mu = 1$, $\lambda = 0.1$, and $c = 0.5$ for each of the control charts for CUSUM, EWMA, and modified EWMA

φ, θ	δ	ARL$_0$=370			ARL$_0$=500		
		CUSUM	EWMA	MEWMA	CUSUM	EWMA	MEWMA
		***b*=4.888**	***l*=0.001461**	***h*=0.526038**	***b*=5.385**	***l*=0.00195**	***h*=0.527244**
$\varphi = 0.2$ $\theta = 0.2$	0.00	370.247	370.261	370.299	500.848	500.312	500.658
	0.01	343.074	331.525	156.855	460.052	447.794	176.564
	0.05	256.821	217.525	46.293	333.002	293.361	47.944
	0.10	184.623	134.030	24.020	230.246	180.407	24.479
	0.25	81.957	39.611	9.461	92.922	52.937	9.539
	0.50	32.568	9.310	4.678	33.749	12.150	4.699
	1.00	12.151	2.150	2.530	12.191	2.540	2.536
	1.25	9.134	1.582	2.150	9.220	1.779	2.154
	1.50	7.359	1.334	1.912	7.484	1.447	1.915
AEQL		**6.530**	**1.594**	**1.369**	**6.762**	**1.945**	**1.374**
PCI		**4.769**	**1.164**	**1.000**	**4.923**	**1.416**	**1.000**
		***b*=3.971**	***l*=0.0009772**	***h*=0.649436**	***b*=4.322**	***l*=0.001303**	***h*=0.650827**
$\varphi = 0.5$ $\theta = 0.7$	0.00	370.432	370.313	370.358	500.170	500.257	500.244
	0.01	346.665	330.199	168.794	466.055	445.860	191.719
	0.05	269.314	213.282	51.880	356.114	287.474	53.941
	0.10	201.658	129.100	27.151	261.603	173.626	27.729
	0.25	97.750	36.552	10.737	120.851	48.768	10.835
	0.50	41.155	8.249	5.282	48.095	10.714	5.307
	1.00	14.823	1.939	2.806	16.335	2.255	2.813
	1.25	10.766	1.465	2.364	11.688	1.621	2.369
	1.50	8.405	1.262	2.086	9.031	1.350	2.089
AEQL		**7.742**	**1.475**	**1.511**	**8.672**	**1.783**	**1.517**
PCI		**5.250**	**1.000**	**1.025**	**5.718**	**1.176**	**1.000**

Table 4. Calculated ARL values using the explicit formula for the SARMA(1,1)$_4$ process in the case of $\mu = 1$, $\lambda = 0.1$, and $c = 0.5$ for each of the control charts for CUSUM, EWMA, and modified EWMA.

ϕ, θ	δ	ARL$_0$=370			ARL$_0$=500		
		CUSUM	EWMA	MEWMA	CUSUM	EWMA	MEWMA
		***b*=3.811**	***l*=0.001616**	***h*=0.526036**	***b*=4.155**	***l*=0.002158**	***h*=0.527242**
$\varphi = 0.9$ $\theta = 0.9$	0.00	370.247	370.261	370.139	500.848	500.312	500.366
	0.01	343.074	331.525	156.826	460.052	447.794	176.528
	0.05	256.821	217.525	46.290	333.002	293.361	47.941
	0.10	184.623	134.030	24.020	230.246	180.407	24.479
	0.25	81.957	39.611	9.460	92.922	52.937	9.538
	0.50	32.568	9.310	4.678	33.749	12.150	4.699
	1.00	12.151	2.150	2.530	12.191	2.540	2.536
	1.25	9.134	1.582	2.150	9.220	1.779	2.154
	1.50	7.359	1.334	1.912	7.484	1.447	1.915
AEQL		**6.530**	**1.594**	**1.369**	**6.762**	**1.945**	**1.374**
PCI		**4.769**	**1.164**	**1.000**	**4.923**	**1.416**	**1.000**
		***b*=4.887**	***l*=0.002186**	***h*=0.722257**	***b*=5.383**	***l*=0.002922**	***h*=0.650827**
$\varphi = 0.3$ $\theta = 0.6$	0.00	370.008	370.061	370.068	500.281	500.235	500.306
	0.01	342.859	332.726	176.050	459.549	449.625	201.212
	0.05	256.675	221.780	55.500	332.687	299.321	57.865
	0.10	184.532	139.116	29.187	230.068	187.447	29.854
	0.25	81.930	42.934	11.555	92.890	57.488	11.668
	0.50	32.563	10.529	5.661	33.751	13.808	5.690
	1.00	12.151	2.410	2.975	12.193	2.892	1.982
	1.25	9.133	1.730	2.494	9.221	1.979	2.499
	1.50	7.358	1.427	2.191	7.484	1.572	2.195
AEQL		**6.529**	**1.735**	**1.599**	**6.762**	**2.137**	**1.493**
PCI		**4.084**	**1.086**	**1.000**	**4.528**	**1.431**	**1.000**

5. Application

This section analyzes the average global temperature in degrees Celsius, relative to a specified base period, using data from the global temperature dataset (https://datahub.io/core/global-temp). The dataset comprises monthly observations from January 2010 to July 2024, represented by a Seasonal Autoregressive Moving Average ($SARMA(1,1)_L$) model.

The IBM SPSS software package fits the model to the temperature data. The results, indicating the suitability of the $SARMA(1,1)_{12}$ model and its corresponding parameters, can be seen in Table 5. Meanwhile, the white noise component following an exponential distribution was verified for its suitability through the one-sample Kolmogorov-Smirnov test, which produced a p-value exceeding 0.05, indicating a good fit.

The model of the real dataset can be expressed as:

$$Y_t = 0.993Y_{t-12} - 0.439\varepsilon_{t-12} + \varepsilon_t, \tag{23}$$

where ε_t is exponentially distributed with a mean of β_0=0.2133.

Table 5. Model fitting for $SARMA(1,1)_{12}$ process for average global temperature (in degree Celsius) relative to a base

Model fit Statistics				
Parameter	**Coefficient**	**Std. Error**	**t-Statistic**	**p-value**
SAR(1)	0.993	0.006	169.791	< 0.001
SMA(1)	0.439	0.096	4.567	< 0.001

The effectiveness of the proposed control chart in monitoring and detecting mean shifts was assessed using a real dataset from the fitted model of average global temperature. Its performance was compared against the classical CUSUM and EWMA control charts. The primary measure of this comparison was the ARL_1 value, where a smaller ARL_1 indicates a faster detection of mean shifts in an out-of-control process.

Table 6 presents the ARL_1 values for both the original and modified EWMA control procedures using the recommended parameter$\lambda = 0{,}1$, obtained through the proposed explicit formula technique. The results demonstrate the superiority of the modified EWMA approach, as it consistently yielded smaller ARL_1 values across all tested shift magnitudes. This reduction in ARL_1 implies that the modified chart can detect smaller temperature deviations more rapidly, which is particularly crucial in long-term environmental monitoring, where early signal identification supports proactive climate responses.

Table 6. Comparison ARL for $SARMA(1,1)_{12}$ process for global temperature in degree Celsius relative to a base period when $\varphi = 0.993$, $\theta = 0.439$, and $\beta_0 = 0.2133$ for the charts relating to CUSUM, EWMA, and modified EWMA on the basis of analytical formulas.

δ	ARL_0=370			ARL_0=500		
	CUSUM (b=0.2625)	**EWMA (l=1.352x10^{-3})**	**MEWMA (h=7.2x10^{-9})**	**CUSUM (b=0.327)**	**EWMA (l=1.4076x10^{-3})**	**MEWMA (h=7.503x10^{-9})**
0.0000	370.460	370.840	370.652	500.218	500.009	500.486
0.0001	369.431	366.056	351.328	498.757	491.947	467.401
0.0005	365.354	347.913	289.368	492.968	461.840	367.579
0.0010	360.342	327.258	235.054	485.855	428.435	287.187
0.0025	345.847	276.052	144.718	465.314	349.385	166.196
0.0050	323.377	215.298	81.257	433.963	262.017	89.476
0.0100	283.996	142.931	36.227	378.190	166.123	38.702
0.0250	198.740	59.428	7.732	259.759	65.383	8.061
0.0500	119.968	22.589	1.933	152.698	24.140	1.974
0.1000	55.644	6.855	1.052	68.008	7.176	1.054
0.2500	15.025	1.734	1.000	17.137	1.767	1.000
0.5000	5.785	1.150	1.000	6.284	1.157	1.000
AEQL	**0.284**	**0.048**	**0.028**	**0.327**	**0.050**	**0.028**
PCI	**10.028**	**1.708**	**1.000**	**11.506**	**1.758**	**1.000**

Values for AEQL and PCI were also determined in order to provide additional performance validation, with the modified EWMA chart achieving a PCI value of 1.000, confirming its superiority, as seen in the earlier simulations. A PCI value equal to one indicates that the chart operates at maximum statistical efficiency, meaning that it maintains the desired false alarm rate while achieving the fastest possible detection of out-of-control conditions. Similarly, the AEQL results further confirm that the modified EWMA chart minimizes detection delay and monitoring cost, underscoring its practicality for sustained environmental applications.

These results emphasize the modified EWMA chart's outstanding capability to identify process shifts under observation. It can be inferred that this chart offers an optimal balance between sensitivity and stability, enabling precise detection of small but meaningful changes in global temperature dynamics. Furthermore, the results highlight the limitations associated with the CUSUM chart, for which the capabilities are somewhat lacking in comparison to the traditional and modified EWMA charts. The CUSUM chart's relatively higher ARL_1 and lower PCI suggest its limited responsiveness in non-industrial, time-dependent systems like global climate data.

The CUSUM chart exhibits difficulties in identifying minor changes in the average global temperature, which, although subtle, can have profound implications for humanity and ecosystems worldwide. Hence, the findings advocate for the adoption of adaptive and data-driven SPC approaches—such as the proposed modified EWMA control chart—as reliable tools for climate trend surveillance, where continuous sensitivity to small mean shifts is essential for timely environmental decision-making.

The anomalies in average global temperature, measured in degrees Celsius relative to the 20th-century average, were extended to forecast the next 12 months (from August 2024 to July 2025) using the SARMA$(1,1)_{12}$ model. The effectiveness of the control chart could be illustrated when graphs were plotted to draw comparisons between the predicted 12-month data points and the original dataset, which includes 187 months of average global temperature data.

Figure 2 illustrates the CUSUM chart performance, whereby a smaller control shift was identified for the relative average global temperature between the 9th to 69th observations and an upper control shift at the 75th and 187th observations.

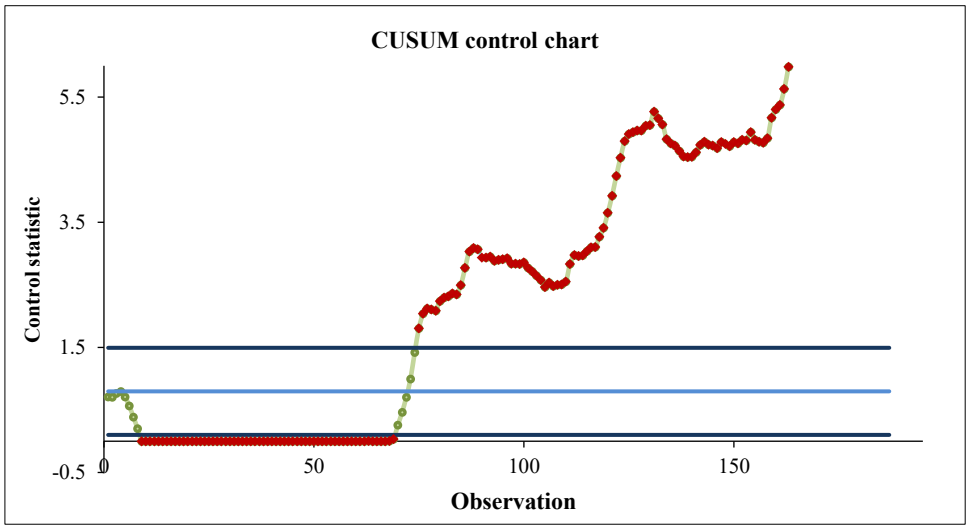

Figure 2. CUSUM chart performance for mean change identification

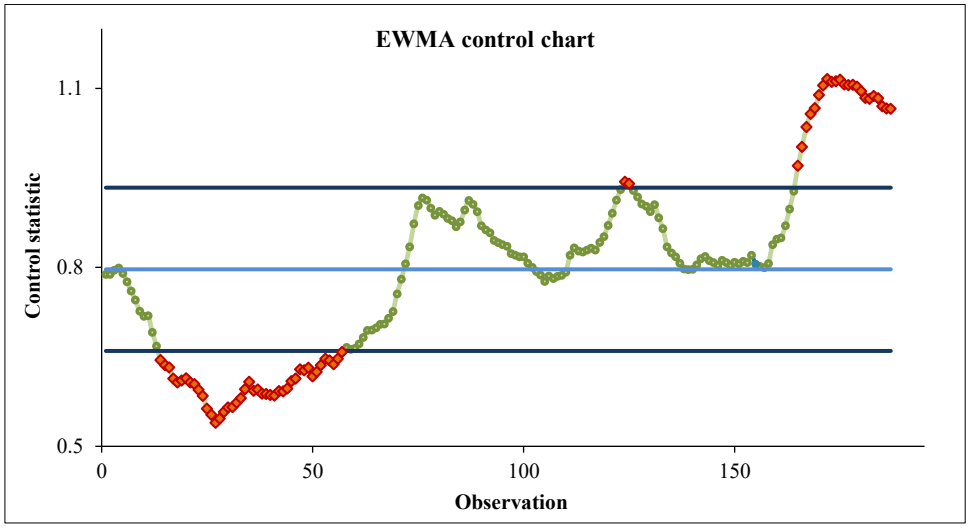

Figure 3. EWMA chart outcomes in detecting mean changes

In contrast, Figure 3 reveals the identification of lower control violations between the 14th and 57th observations for the original EWMA chart, and between identified lower control violations in the 124th and 125th and between the 165th and so on observations.

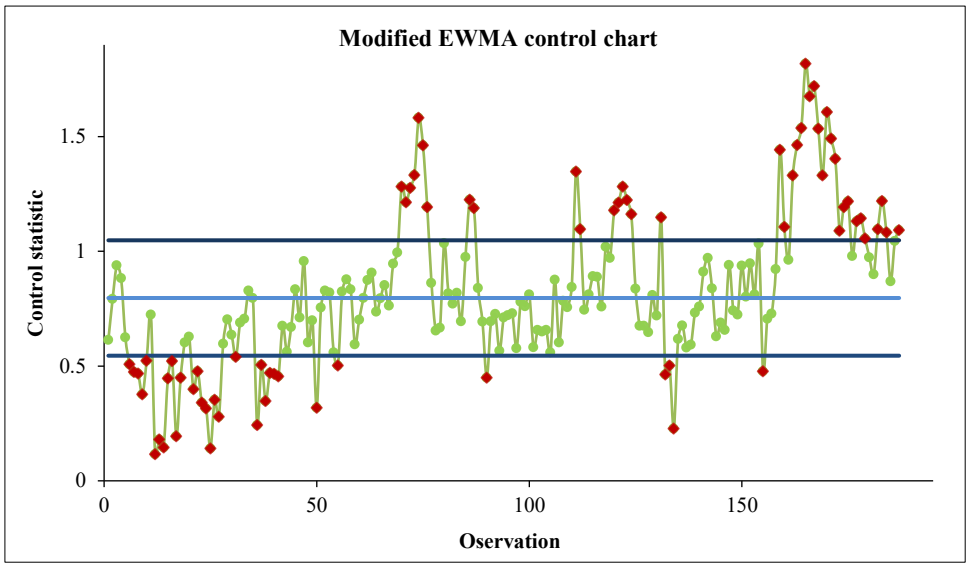

Figure 4. Modified EWMA chart outcomes for mean change identification

Figure 4 highlights the enhanced effectiveness offered by the modified EWMA control chart, which was capable of identifying violations of the lower control limit for the 6th to 10th, 12rd to 18th, 21st to 27th, 31st, 36th to 341st, 50th, 55th, 90th, 132rd to 134th, and 155th observations, and upper limit violations at the 70th to 76th, 86th to 87th, 120th to 124th, 131st, 159th 160th, 162rd to 175th, 177th to 179th, 182rd to 184th, and 187th observations.

An initial change in the global mean temperature was rapidly detected using the modified EWMA control chart, while the other standard control charts lagged in their response, thus indicating the superior sensitivity and response time of the modified EWMA chart.

The forecast data for global average temperature indicates a clear upward trend, reflecting the ongoing rise in global temperatures. This rise is a key factor contributing to climate change, which has widespread impacts on the environment and all forms of life. As global temperatures continue to climb, the planet's ecosystems experience major disturbances, resulting in more frequent and intense weather events like hurricanes, heat waves, and droughts.

In this regard, statistical process control (SPC) techniques, including the conventional CUSUM and EWMA, along with modified EWMA control charts, can be applied to offer significant advantages in observing and predicting current and future trends in temperatures worldwide. SPC methods are traditionally used in manufacturing and quality control. Still, the capacity to identify minor changes arising in process data ensures their importance for environmental monitoring, particularly in identifying subtle changes in global temperature patterns before they become critical.

By applying these control charts to climate data, researchers can efficiently monitor temperature variations and identify any signals indicating that the process might be moving out-of-control as a consequence of unusual increases or falls in temperature. The early detection of these trends allows for timely interventions and improved climate forecasting models, which are essential for preparing and mitigating the adverse effects of global warming. Furthermore, SPC techniques offer a robust statistical framework to assess and predict future climate behavior, which is critical for developing coordinated approaches to address the effects of climate change over the longer term.

As indicated by the forecast, the global temperature increase will affect the climate change phenomenon, impacting ecosystems, human health, food security, and all living organisms. Global warming can result in glacial melting and a reduction in the ice caps at the poles, causing sea levels to rise with the potential to bring about catastrophic consequences for populations inhabiting low-lying coastal regions. Additionally, shifts in temperature patterns disrupt agricultural systems, diminish biodiversity, and amplify the occurrence of extreme weather events.

Statistical process control methods are instrumental in improving our understanding of these complex processes. They allow for the continuous monitoring of global temperatures and help forecast future climate scenarios with greater accuracy, thus providing a scientific basis for policy decisions and climate mitigation strategies. The early warning capabilities offered by these control charts enable governments, researchers, and environmental agencies to take proactive measures, thereby minimizing the adverse effects of global temperature rises and contributing to the worldwide fight against climate change.

6. Discussion

This research aimed to develop and assess the modified EWMA control chart, specifically designed to identify mean changes in an SARMA$(1,1)_L$ model, which incorporates exponential white noise. The control chart was tested using a real-world dataset of global mean temperature anomalies spanning from January 2010 to July 2024. An important factor contributing to the effectiveness of the chart lies in the choice of the smoothing parameter (λ). In this study, λ was set to 0.10, which was empirically determined to provide an optimal balance between sensitivity and stability in detecting small process shifts. Prior research by Paichit & Peerajit [41] and Supharakonsakun et al. [35] demonstrated that a modified EWMA chart with $\lambda = 0.10$ outperformed the standard version, while Supharakonsakun & Areepong [42] reported that $\lambda = 0.20$ yielded the most efficient detection across multiple shift magnitudes. These findings, consistent with those of Supharakonsakun et al. [36], reinforce the configuration adopted in this study and confirm that higher λ values enhance responsiveness to subtle changes in autocorrelated processes.

The explicit formula method for deriving ARL values allowed for rapid and accurate computation, enhancing the practicality of the chart for real-time monitoring. Using the optimized parameter$\lambda = 0.1$, the modified EWMA chart consistently outperformed baseline EWMA and CUSUM charts in its ability to identify minor changes, confirmed by the recording of lower ARL_1 values. The %PRA method also confirmed that the explicit formula generated accurate ARL values, while the performance of the modified EWMA chart showed greater efficiency than was the case for alternative approaches. Together, these enhancements, the explicit ARL formulation, and optimized smoothing parameter, solidify the modified EWMA chart as a robust and sensitive tool capable of detecting subtle process changes in complex, real-world data environments such as global temperature monitoring.

The study also extended its analysis to forecast future global temperature anomalies using the SARMA$(1,1)_{12}$ model, yielding an R^2 value of 0.847. The forecasted upward trend in global temperature underscores the urgent need for effective monitoring tools, especially in light of the worldwide climate crisis. With its optimized parameters, the modified EWMA chart can identify changes in worldwide temperature patterns at an early stage with a high degree of reliability. This enhanced capability is vital for environmental monitoring, helping policymakers respond more swiftly to climate-related changes.

The flexibility of the proposed SPC framework also allows for potential extension to multivariate temperature indices, such as the joint analysis of land and ocean temperature anomalies. By incorporating multivariate control structures (e.g., MEWMA or Hotelling's T^2-based approaches), the framework can monitor correlated climate indicators simultaneously, thereby capturing the complex interdependencies inherent in global temperature systems. Such an extension would enhance the applicability of the model to complex climate systems, where interdependence between environmental variables plays a critical role.

In conclusion, the modified EWMA control chart, with its optimized parameters and explicit formula derived ARL values, offers significant advantages for monitoring autocorrelated data. Its alignment with previous empirical findings validates the robustness of the chosen parameterization and modeling structure. Its adaptability to multivariate contexts further broadens its potential for climate monitoring applications. The superior performance of the proposed approach in detecting small mean shifts demonstrates its relevance in addressing global temperature variability, where timely detection and intervention are vital for effective climate mitigation strategies.

7. Conclusion

This study proposed a modified EWMA control chart tailored to detect subtle mean shifts in autocorrelated processes characterized by the SARMA$(1,1)_L$ model with exponential white noise. By introducing an explicit analytical formulation of the Average Run Length (ARL), the method achieves both computational efficiency and numerical precision, overcoming the limitations of simulation-based and iterative numerical approaches. The modified EWMA chart consistently exhibited lower ARL_1 values across various scenarios, outperforming conventional EWMA and CUSUM charts and demonstrating superior sensitivity to small and moderate process shifts. Furthermore, the optimized smoothing parameter ($\lambda = 0.10$) was empirically validated to provide an effective balance between responsiveness and stability, reinforcing findings from prior literature. Together, these results highlight the proposed chart as a robust, efficient, and analytically sound tool for real-time process monitoring.

The practical application to global mean temperature anomalies further confirmed the capability of the chart in detecting early signals of climate variation. Using the SARMA$(1,1)_{12}$ model, the analysis achieved an R^2 value of 0.847, indicating a reliable fit and reflecting the upward trend in global temperatures, a phenomenon of critical concern. This result underscores the relevance of advanced statistical monitoring tools in environmental and climate-related applications. Future research may extend this framework toward multivariate structures, such as MEWMA or Hotelling's T^2-type charts, to jointly monitor interconnected climate indicators. Overall, the modified EWMA control chart, with its explicit ARL formulation, offers a significant advancement in statistical process control, combining analytical rigor, computational practicality, and real-world applicability for complex time-dependent data systems.

8. Declarations

8.1. Author Contributions

Conceptualization, Y.S. and Y.A.; methodology, Y.S.; software, Y.S, K.S., and Y.A.; validation, Y.S. and Y.A.; formal analysis, Y.S.; investigation, Y.S.; resources, Y.S.; data curation, Y.A.; writing—original draft preparation, Y.S.; writing—review and editing, Y.S.; visualization, Y.A.; supervision, Y.A.; project administration, Y.S.; funding acquisition, Y.S. All authors have read and agreed to the published version of the manuscript.

8.2. Data Availability Statement

The data presented in this study are available in the article.

8.3. Funding

This project is funded by National Research Council of Thailand (NRCT): Contract no. N42A670894.

8.4. Institutional Review Board Statement

Not applicable.

8.5. Informed Consent Statement

Not applicable.

8.6. Declaration of Competing Interest

The authors declare that they have no known competing financial interests or personal relationships that could have appeared to influence the work reported in this paper.

9. References

[1] Wang, J., Yan, M., Gao, H., Lu, X., & Kan, B. (2017). Vibrio cholerae colonization of softshelled turtles. Applied and Environmental Microbiology, 83(14), 00713–17. doi:10.1128/AEM.00713-17.

[2] Jian-Bin, H., Shao-Wu, W., Yong, L., Zong-Ci, Z., & Xin-Yu, W. (2012). Debates on the Causes of Global Warming. Advances in Climate Change Research, 3(1), 38–44. doi:10.3724/sp.j.1248.2012.00038.

[3] Dhillon, R. S., & von Wuehlisch, G. (2013). Mitigation of global warming through renewable biomass. Biomass and Bioenergy, 48, 75–89. doi:10.1016/j.biombioe.2012.11.005.

[4] Florides, G. A., & Christodoulides, P. (2009). Global warming and carbon dioxide through sciences. Environment International, 35(2), 390–401. doi:10.1016/j.envint.2008.07.007.

[5] Abas, N., Kalair, A. R., Khan, N., Haider, A., Saleem, Z., & Saleem, M. S. (2018). Natural and synthetic refrigerants, global warming: A review. Renewable and Sustainable Energy Reviews, 90, 557–569. doi:10.1016/j.rser.2018.03.099.

[6] Anderson, T. R., Hawkins, E., & Jones, P. D. (2016). CO2, the greenhouse effect and global warming: from the pioneering work of Arrhenius and Callendar to today's Earth System Models. Endeavour, 40(3), 178–187. doi:10.1016/j.endeavour.2016.07.002.

[7] Intergovernmental Panel on Climate Change. (2014). Climate Change 2013 – The Physical Science Basis. Cambridge University Press, Cambridge, United Kingdom. doi:10.1017/cbo9781107415324.

[8] Neumann, B., Vafeidis, A. T., Zimmermann, J., & Nicholls, R. J. (2015). Future coastal population growth and exposure to sea-level rise and coastal flooding - A global assessment. PLoS ONE, 10(3), 118571. doi:10.1371/journal.pone.0118571.

[9] Kurane, I. (2010). The effect of global warming on infectious diseases. Osong Public Health Research Perspectives, 1(1), 4–9. doi:10.1016/j.phrp.2010.12.004.

[10] Vucijak, B., Midzic Kurtagic, S., Ceric, A., Kupusovic, T., & Spago, S. (2012). Assessment of Climate Change Effects to Precipitation Patterns using Statistical Process Control Methods. Proceedings of the 23rd International DAAAM Symposium 2012, 0277–0280. doi:10.2507/23rd.daaam.proceedings.064.

[11] Vučijak, B., Kupusović, T., Midžić-Kurtagić, S., Silajdžić, I., & C′erić, A. (2014). Evaluation of the climate change effects to the precipitation patterns in the selected Bosnia and Herzegovina cities. Thermal Science, 18(3), 787–798. doi:10.2298/TSCI1403787V.

[12] Cornwell, D., Brown, R., & McTigue, N. (2015). Controlling lead and copper rule water quality parameters. Journal - American Water Works Association, 107(2), E86–E96. doi:10.5942/jawwa.2015.107.0011.

[13] Supharakonsakun, Y., Areepong, Y., & Sukparungsee, S. (2020). The performance of a modified EWMA control chart for monitoring autocorrelated PM2.5 and carbon monoxide air pollution data. PeerJ, 8, e10467. doi:10.7717/peerj.10467.

[14] Arciszewski, T. J. (2023). A Review of Control Charts and Exploring Their Utility for Regional Environmental Monitoring Programs. Environments, 10(5), 78. doi:10.3390/environments10050078.

[15] Griffith, D. A., & Plant, R. E. (2022). Statistical Analysis in the Presence of Spatial Autocorrelation: Selected Sampling Strategy Effects. Stats, 5(4), 1334–1353. doi:10.3390/stats5040081.

[16] Wang, M., Gao, H., Wang, Z., Yue, K., Zhong, C., Zhang, G., & Wang, J. (2024). Correlation between Temperature and the Posture of Transmission Line Towers. Symmetry, 16(10), 1270. doi:10.3390/sym16101270.

[17] Ferguson, J. M., Carvalho, F., Murillo-García, O., Taper, M. L., & Ponciano, J. M. (2016). An updated perspective on the role of environmental autocorrelation in animal populations. Theoretical Ecology, 9(2), 129–148. doi:10.1007/s12080-015-0276-6.

[18] Page, E. S. (1954). Continuous Inspection Schemes. Biometrika, 41(1/2), 100. doi:10.2307/2333009.

[19] Roberts, S. W. (1959). Control Chart Tests Based on Geometric Moving Averages. Technometrics, 1(3), 239–250. doi:10.1080/00401706.1959.10489860.

[20] Aslam, M., Rao, G. S., Khan, N., & Al-Abbasi, F. A. (2019). EWMA control chart using repetitive sampling for monitoring blood glucose levels in type-II diabetes patients. Symmetry, 11(1), 57. doi:10.3390/sym11010057.

[21] rivastava, M. S., & Wu, Y. (1993). Comparison of EWMA, CUSUM and Shiryayev-Roberts Procedures for Detecting a Shift in the Mean. The Annals of Statistics, 21(2), 1176349142. doi:10.1214/aos/1176349142.

[22] Wardell, D. G., Moskowitz, H., & Plante, R. D. (1994). Run-length distributions of special-cause control charts for correlated processes. Technometrics, 36(1), 3–17. doi:10.1080/00401706.1994.10485393.

[23] Jiang, W., Tsui, K. L., & Woodall, W. H. (2000). A new SPC monitoring method: The ARMA chart. Technometrics, 42(4), 399–410. doi:10.1080/00401706.2000.10485713.

[24] Carson, P. K., & Yeh, A. B. (2008). Exponentially weighted moving average (EWMA) control charts for monitoring an analytical process. Industrial and Engineering Chemistry Research, 47(2), 405–411. doi:10.1021/ie070589b.

[25] Han, S. W., Tsui, K. L., Ariyajuny, B., & Kim, S. B. (2010). A comparison of CUSUM, EWMA, and temporal scan statistics for detection of increases in poisson rates. Quality and Reliability Engineering International, 26(3), 279–289. doi:10.1002/qre.1056.

[26] Abbasi, S. A., Riaz, M., Miller, A., Ahmad, S., & Nazir, H. Z. (2015). EWMA Dispersion Control Charts for Normal and Non-normal Processes. Quality and Reliability Engineering International, 31(8), 1691–1704. doi:10.1002/qre.1702.

[27] John, B., & Subhani, S. M. (2020). A modified control chart for monitoring non-normal characteristics. International Journal of Productivity and Quality Management, 29(3), 309–328. doi:10.1504/IJPQM.2020.105990.

[28] Khan, Z., Gulistan, M., Chammam, W., Kadry, S., & Nam, Y. (2020). A New Dispersion Control Chart for Handling the Neutrosophic Data. IEEE Access, 8, 96006–96015. doi:10.1109/ACCESS.2020.2995998.

[29] Vanbrackle, L. N., & Reynolds, M. R. (1997). EVVMA and cusum control charts in the presence of correlation. Communications in Statistics - Simulation and Computation, 26(3), 979–1008. doi:10.1080/03610919708813421.

[30] Fu, J. C., Spiring, F. A., & Xie, H. (2002). On the average run lengths of quality control schemes using a Markov chain approach. Statistics & Probability Letters, 56(4), 369–380. doi:10.1016/S0167-7152(01)00183-3.

[31] Khoo, M. B. C., Castagliola, P., Liew, J. Y., Teoh, W. L., & Maravelakis, P. E. (2016). A Study on EWMA charts with runs rules—the Markov chain approach. Communications in Statistics - Theory and Methods, 45(14), 4156–4180. doi:10.1080/03610926.2014.917187.

[32] Supharakonsakun, Y. (2024). Bayesian Control Chart for Number of Defects in Production Quality Control. Mathematics, 12(12). doi:10.3390/math12121903.

[33] Zhang, J., Li, Z., & Wang, Z. (2009). Control chart based on likelihood ratio for monitoring linear profiles. Computational Statistics and Data Analysis, 53(4), 1440–1448. doi:10.1016/j.csda.2008.12.002.

[34] Peerajit, W. (2023). Developing Average Run Length for Monitoring Changes in the Mean on the Presence of Long Memory under Seasonal Fractionally Integrated MAX Model. Mathematics and Statistics, 11(1), 34–50. doi:10.13189/ms.2023.110105.

[35] Supharakonsakun, Y., Areepong, Y., & Sukparungsee, S. (2020). The exact solution of the average run length on a modified EWMA control chart for the first-order moving-average process. ScienceAsia, 46(1), 109. doi:10.2306/scienceasia1513-1874.2020.015.

[36] Supharakonsakun, Y., Areepong, Y., & Sukparungsee, S. (2020). Monitoring the Process Mean of a Modified Ewma Chart for Arma(1,1) Process and Its Application. Suranaree Journal of Science and Technology, 27(4), 1–11.

[37] Supharakonsakun, Y. (2021). Comparing the Effectiveness of Statistical Control Charts for Monitoring a Change in Process Mean. Engineering Letters, 29(3).

[38] Patel, A. K., & Divecha, J. (2011). Modified exponentially weighted moving average (EWMA) control chart for an analytical process data. Journal of Chemical Engineering and Materials Science, 2(1), 12-20.

[39] Khan, N., Aslam, M., & Jun, C. (2016). Design of a Control Chart Using a Modified EWMA Statistic. Quality and Reliability Engineering International, 33(5), 1095–1104. doi:10.3390/technologies6040108.

[40] Alevizakos, V., Chatterjee, K., & Koukouvinos, C. (2020). The triple exponentially weighted moving average control chart. Quality Technology & Quantitative Management, 1–29. doi:10.1002/qre.2999.

[41] Paichit, P., & Peerajit, W. (2022). The average run length for continuous distribution process mean shift detection on a modified EWMA control chart. Asia-Pacific Journal of Science and Technology, 27(6), 1-13.

[42] Supharakonsakun, Y., & Areepong, Y. (2022). Design and Application of a Modified EWMA Control Chart for Monitoring Process Mean. Applied Science and Engineering Progress, 15(4), 5198. doi:10.14416/j.asep.2021.06.007.

Appendix I

Table A1. Pseudocode Representation of the Proposed Explicit Formula and NIE Procedure

Step	Description
1. Model Specification	Define the Seasonal Autoregressive Moving Average model SARMA(1,1)_L incorporating exponential white noise as described in Eq. (9). Specify AR and MA coefficients (ϕ, θ) and seasonal lag L.
2. Modified EWMA Statistic Construction	Formulate the modified EWMA statistic for SARMA(1,1)_L data as shown in Eq. (10), assuming one-sided monitoring with LCL = 0.
3. Control Limit Definition	Set upper control limit (UCL) and identify in-control (IC) and out-of-control (OOC) states as described in Eq. (11).
4. Derivation of Integral Equation	Establish the Fredholm integral equation of the second kind (Eq. 12–13) representing the ARL relationship under exponential noise.
5. Explicit Formula Solution	Derive the explicit formula for ARL using analytical integration based on the exponential distribution assumption (Eq. 14–16).
6. Numerical Verification (NIE Method)	Approximate ARL values numerically using the Numerical Integral Equation (NIE) approach and Gauss–Legendre quadrature, following Eq. (17–19).
7. %PRA Evaluation	Compute the Percentage Relative Accuracy (%PRA) to compare the explicit ARL formula with numerical NIE results, ensuring precision of the analytical solution.